INSIGHTS INTO THE CHEMICAL CHARACTERISTICS OF ATMOSPHERIC AEROSOLS FROM URBAN-INDUSTRIAL AND RURAL SITES IN SOUTH-EAST OF POLAND DURING WINTER

Mirosław Szwed [1], Rafał Kozłowski [1], Witold Żukowski [2], Saliou Mbengue [3], Lenka Suchánková [3], Roman Prokes [3,4]

[1] Institute of Geography and Environmental Sciences, Jan Kochanowski University, Kielce, Poland
[2] Faculty of Chemical Engineering and Technology, Cracow University of Technology, Cracow, Poland
[3] Global Change Research Institute of the Czech Academy of Sciences, Brno, Czech Republic
[4] RECETOX, Faculty of Science, Masaryk University, Brno, Czech Republic

Manuscript received: August 16, 2022
Revised version: April 22, 2023

Szwed M., Kozłowski R., Żukowski W., Mbengue S., Suchankova L., Prokes R., 2023. Insights into the chemical characteristics of atmospheric aerosols from urban-industrial and rural sites in south-east of Poland during winter. *Quaestiones Geographicae* 42(3), Bogucki Wydawnictwo Naukowe, Poznań, pp. 89–99. 6 figs, 2 tables.

Abstract: This study focusses on a short-term characterisation of atmospheric aerosols from three locations in south-east of Poland with different land use characteristics, population density and sources of pollution (Katowice: urban-industrial; Strzyżowice near Lublin: rural; Kielce: urban). Twenty-four hour $PM_{2.5}$ and PM_{10} samples were collected on the quartz filter and their chemical compositions were monitored and measured using OCEC thermo-optical analysis and scanning electron microscopy-energy dispersive X-ray spectrometry (SEM-EDS). The highest concentrations of $PM_{2.5}$ and PM_{10} were measured at the urban-industrial area in Katowice (29.6 $\mu g \cdot m^{-3}$ and 31.0 $\mu g \cdot m^{-3}$, respectively), whereas the highest organic carbon (OC) and elemental carbon (EC) levels were observed at the Kielce urban site (23.3 ± 4.2 µg and 3.6 ± 0.3 µg, respectively). The lowest values were obtained at the rural site for $PM_{2.5}$ (10.4 ± 2.7 $\mu g \cdot m^{-3}$) and PM_{10} (11.8 ± 2.7 $\mu g \cdot m^{-3}$) and for OC (17.8 ± 1.6 µg) and EC (1.0 ± 0.1 µg). SEM-EDS analysis of samples from Kielce allows identification of internal chemical mixtures of carbon, silicon, calcium, chlorine, sodium and aluminium.

Key words: atmospheric aerosol, elemental-organic carbon, industrial emissions, single particle mass spectrometry

Corresponding author: Mirosław Szwed; miroslaw.szwed@ujk.edu.pl

Introduction

Ambient air pollution is one of the basic threats to the natural environment and human health (Kampa, Castanas 2008, Peel et al. 2012, Eguiluz-Gracia et al. 2020). Atmospheric aerosols consist of a complex mixture of different chemical components including inorganic species (salts, metals) and carbonaceous compounds emitted by a variety of anthropogenic and natural sources (Seinfeld 2003, Mbengue et al. 2014, 2017, Szwed et al. 2020, Rybiński et al. 2021). Despite the significant efforts made during recent years for the reduction of air pollutant emissions from most kinds of anthropogenic sources in the European Union, local and long-term exceedances of air quality limit values remain a major public health problem in urban areas (Cichowicz et al. 2017). Poor air quality in urban areas is mainly related to the large variability of sources including

https://doi.org/10.14746/quageo-2023-0025
ISSN 2082-2103, eISSN 2081-6383

traffic (worn tyres, vehicle exhaust and road dust), avenues of economic activity (commercial establishments) and municipal-housing sectors (residential heating, construction, and industrial activities) (Paraschiv et al. 2019).

Carbonaceous aerosols, including particulate organic carbon (OC) and elemental carbon (EC), are the main components of atmospheric aerosols and play an important role in atmospheric chemistry, climate change and public health due to their physical and environmental properties (Mbengue et al. 2015). EC is the product of incomplete combustion of fossil fuels in transport and energy production, as well as wood and biomass burning from residential heating and agricultural activities. Primary organic carbon (POC) can be emitted from anthropogenic or biogenic sources, while secondary organic carbon (SOC) can be produced as a result of atmospheric oxidation of reactive organic gases and subsequent gas-to-particle conversion processes.

Among the filter-based measurement techniques, the thermo-optical analysis has been widely used for determination of OC and EC in ambient aerosol (Cavalli et al. 2010, Mbenque et al. 2018). Scanning electron microscopy-energy dispersive X-ray spectrometry (SEM-EDS) is an efficient technique for the characterisation of properties (size, morphology and elemental composition) of individual particles (Arndt et al. 2016). The present study aims to provide information on the chemical properties and potential sources of atmospheric aerosols from urban and rural areas in Poland with different profiles of economic activity.

Materials and methods

Study areas

Air pollutants measurements were carried out in the first quarter of 2022, during the season that necessitates artificial, at three sites in southern (Katowice) and south-eastern (Kielce and Strzyżowice) Poland (Fig. 1).

Katowice (289,200 inhabitants) is one of the cities that form the Silesian conurbation, in the most industrialised and most densely populated part of the country (1755.9 people · km^{-2}) (GUS 2022). The prevailing wind directions (Table

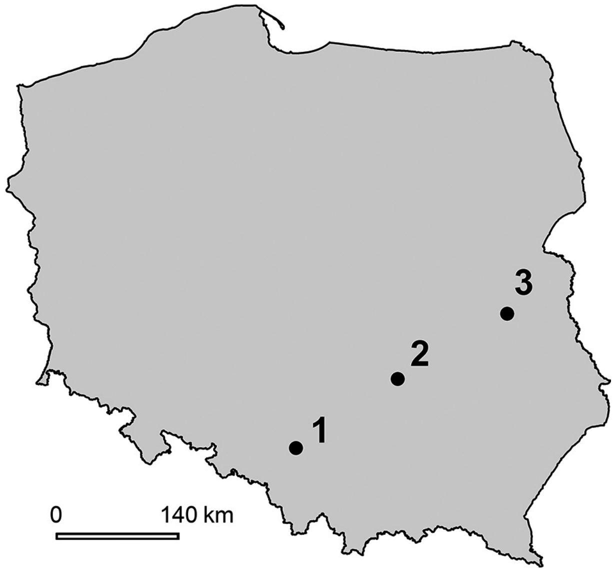

Fig. 1. Location of the sampling sites (1 – Katowice, 2 – Kielce, 3 - Strzyżowice).

1) are mostly SW with average wind speed of 2.6 m · s^{-1}. Kielce, the capital of the Świętokrzyskie Voivodeship, is inhabited significantly sparser (193,400 inhabitants) with an average density of 1764.7 people · km^{2}. The sampling site was mostly affected by NE, 0.9 winds (speed in m · s^{-1}). Strzyżowice represents a rural site in an agricultural landscape (255 inhabitants) mainly affected by SSW, 3.1 winds (speed in m · s^{-1}). The field campaigns in selected locations were conducted in mild winter conditions, mostly characterised by positive daily average ambient temperatures (Turpin et al. 2000). The biggest daily temperature drop (T_{min} = −4.4°C) was recorded in Kielce, during the influx of arctic air masses (Table 1). At Strzyżowice and Katowice, no temperatures below 0°C were measured.

Aerosol sampling

In this study, 24-h samples were collected at Katowice (25–26.01.2022), Kielce (9–10.02.2022) and Strzyżowice (9–10.03.2022) using a fine dust aerosol spectrometer (Palas Fidas 200S, Germany) (Table 1). The device is an optical aerosol spectrometer that determines the particle size of a single molecule using scattered light according to the Lorenz–Mie law. It operates in the measuring range from 1 µg · m^{-3} to 1000 µg · m^{-3}. The instrument is a part of the mobile measurement platform of the Research and Analysis Center of Jan Kochanowski University, and it is accredited

Table 1. Meteorological conditions during aerosol sampling.

Site location	Sampling period	Aerosol measurements	Weather			
			Temperature	Relative humidity	Air pressure	Prevaling wind direction and speed
			[°C]	[%]	[hPa]	[m s^{-1}]
Katowice (urban-industrial), 50°14'15.8"N, 18°59'28.8"E	25–26.01.22	$PM_{2.5}$, PM_{10}, TC, Elemental carbon, Organic carbon	0.5±0.1	97.1±1.8	990.3±0.6	SW, 2.6
Strzyżowice (rural), 51°34'09.8"N, 22°00'22.0"E	9–10.02.22	$PM_{2.5}$, PM_{10}, TC, Elemental carbon, Organic carbon	7.3±1.0	78.0±5.7	1004.6±1.1	SSW, 3.1
Kielce (urban), 50°52'00.0"N, 20°38'20.8"E	9–10.03.22	$PM_{2.5}$, PM_{10}, TC, Elemental carbon, Organic carbon, Elemental composition	1.2±3.9	64.4±13.11	991.2±9.6	NE, 0.9

for suspended dust measurements by the Polish Accreditation Committee No. AB1622 (PCA 2021). The pneumatic system of the device operates with the flow 4.8 l · min^{-1}, and the sampling inlet prevents the intake of particles larger than 20 µm. The measurement uncertainty was for $PM_{2.5}$ was 13% for concentrations ≥18 µg · m^{-3} and 12% for concentrations <18 µg · m^{-3}. For PM_{10}, the uncertainty was 11% for concentrations ≥30 µg · m^{-3} and 7% for concentrations <30 µg · m^{-3}. The measurement platform is equipped with the meteorological station Vaisala WXT536 (Helsinki, Finland). Each sampling campaign lasted for 24 h; dates and precise sites' locations are given in Figure 1.

Analysis of carbonaceous aerosols

The concentrations of carbonaceous aerosols were determined in PM collected on a 47 mm quartz fibre filter (Whatman®, Cytiva) installed in the dust monitor pneumatic system. Four samples (13 mm in diameter) were punched from each filter, and analysed for OC, EC and TC (OC + EC) with a semi-continuous OCEC aerosol thermal-optical analyser (Sunset Laboratories model 4, Tigard Oregon, USA), according to the shortened EUSAAR-2 protocol (Cavalli et al. 2010, Mbengue et al. 2018). After introducing the sample into the instrument, the particulate laden filter was heated in an ultra-pure helium atmosphere in four incremental temperature steps from 200°C to 650°C. The thermally desorbed OC fractions were converted to CO_2 gas in a manganese dioxide (MnO_2) oxidation oven and measured directly in an independent, non-dispersive infrared detector (NDIR) system.

A second temperature ramp (500–850°C) was initiated in an oxygen and helium mixture, and both the original EC and the pyrolysed carbon (PC) produced from the OC during the first temperature increase were converted to CO_2 and detected by NDIR. Correction for PC was performed by monitoring laser absorbance (red 660 nm) through the quartz fibre filter during sample analysis. A laboratory blank was measured, and control calibrations were performed with sucrose solution before and after each sample to check the stability of the instrument.

It is worth nothing that for OCEC field analysis, the instrument is equipped with a carbon parallel plate diffusion denuder (ex Sunset Lab., Tigard Oregon, USA) to remove volatile organic compounds that may be adsorbed on the quartz fibre filter, causing positive artefacts in OC measurement (Turpin et al. 2000). Therefore, in the absence of a similar system during our sampling campaigns, the OC values could be overestimated (Table 1).

SEM-EDS characterisation

The EDS analysis of the surface of quartz filter in Kielce allowed determining the elemental composition (qualitative analysis) and the percentage of micro components (quantitative analysis) of deposited particles. The specificity and limitations of this analytical method should be considered when interpreting the results of the EDS analysis (Szwed et al. 2021). The graphical images resulting from this analysis are created in parallel with the SEM image of the tested sample surface. Information on the composition of the surface and the arrangement of individual elements is the result of the measured intensity and X-ray energy, which depends on the excitation of the core-shell electron of the sample. It should be remembered that the electrons used to create the SEM image (as well as obtain EDS data) penetrate the material to different depths depending on the type of matrix, but not more than a few micrometres. In addition, based on the raw data from the X spectrum assigned to each pixel of the SEM image, quantitative data can be obtained, allowing the comparison of the mass (or molar) fractions of elements in the subsurface layer of the scanned area. For this purpose, the area for this analysis is selected, delimited by a circle or a rectangle, and X-ray intensity for individual wavelengths is integrated. Integration is calculated for the different elements (all detected or selected arbitrarily by the operator), and the results are normalised, so that the sum of shares is 100%. This method could provide information regarding the nature of the tested material, the particle morphology and the potential sources of individual components.

Auxiliary data

Meteorological parameters (temperature, RH, air pressure and wind speed and direction) were monitored by Vaisala WXT536 (Helsinki, Finland). The obtained results were controlled using a Lat CHOT-2BM thermohygrometer (Katowice, Poland) certified by an accredited calibration laboratory (AP 053). The origins of the air masses affecting the different sampling sites have been investigated using Back Trajectory (BT) analysis (Stein et al. 2015, Rolph et al. 2017). The meteorological data used for BT calculation were downloaded from the Global Data Assimilation System (GDAS1) Archive Information. Forty-eight hour backward trajectories of air masses arriving every 6 h at 50 m above ground level (a.g.l.) were calculated using the HYSPLIT 4 model.

Results

During the campaigns, the permissible standards for the concentration of $PM_{2.5}$ and PM_{10} were not exceeded at all three locations (Dziennik Ustaw 2021, WHO 2021). The highest daily values were recorded at the urban-industrial site in Katowice ($PM_{2.5}$, 29.6 $\mu g \cdot m^{-3}$ and PM_{10}, 31.0 $\mu g \cdot m^{-3}$), whereas the lowest values were observed at the rural site in Strzyżowice (10.4 $\mu g \cdot m^{-3}$ and 11.8 $\mu g \cdot m^{-3}$, respectively) (Table 2). At Kielce (urban) and Katowice, the diurnal pattern of $PM_{2.5}$ and PM_{10} concentrations was more visible (Fig. 2), with a peak in the morning (7.00–9.00) and the second peak in the evening (18.00–21.00). The highest concentrations were observed during night time at all sites (Figs 2 and 3). At the rural site, the diurnal variation is less pronounced.

In the case of carbonaceous aerosols, the highest values were measured in Kielce (EC, 3.6 µg; OC, 23.3 µg; and TC, 27.0 µg). The lowest concentrations were measured at the rural site (EC, 1.0 µg; OC, 17.8 µg; and TC, 18.7 µg).

The SEM-EDS analysis provided information on the particle size and their chemical composition, both qualitatively and quantitatively. The analysis was carried out for two independent areas of the sample, where the dust concentration was the highest (A and B on Fig. 3A and 3B, respectively).

The analysis showed the presence of internally mixed particles. The biggest particles had an oval shape, and their largest size was 18.4 µm in the area A and 20.6 µm in the area B. There were also many smaller particles in the field of view of the camera, with an average size between 3 µm and 10 µm.

The EDS analysis (Fig. 4A and 4B for area A and area B, respectively) shows the automatically identified elements with individual colours, resulting from the presence of specific peaks in the energy spectrum of X-rays generated during the analysis. As could be expected, Si dominates

Table 2. Total content of dust and carbon parameters (TC, OC and EC) for different samples.

Sites	Dust $PM_{2.5}$	Dust PM_{10}	Total content of dust TC	Organic carbon OC	Elemental carbon EC
	[$\mu g \cdot m^{-3}$]		[µg]		
Katowice (urban-industrial)	29.6±11.2	31.0±11.9	21.9±1.9	19.7±1.7	2.2±0.2
Strzyżowice (rural)	10.4±2.7	11.8±2.7	18.7±1.5	17.8±1.6	1.0±0.1
Kielce (urban)	13.3±4.9	20.8±8.6	27.0±4.1	23.3±4.2	3.6±0.3

among the detected elements. In this case, the signal comes mainly from the filter material; therefore, this element was omitted in further qualitative and quantitative analysis to eliminate measurement uncertainties in the data interpretation.

A clear differentiation of the elemental composition of individual dust particles can be observed. Figure 5A and 5B show the particles that clearly generate a signal from chlorine and sodium (x) and those that generate a signal from calcium (o). Subsequently, the observed filter

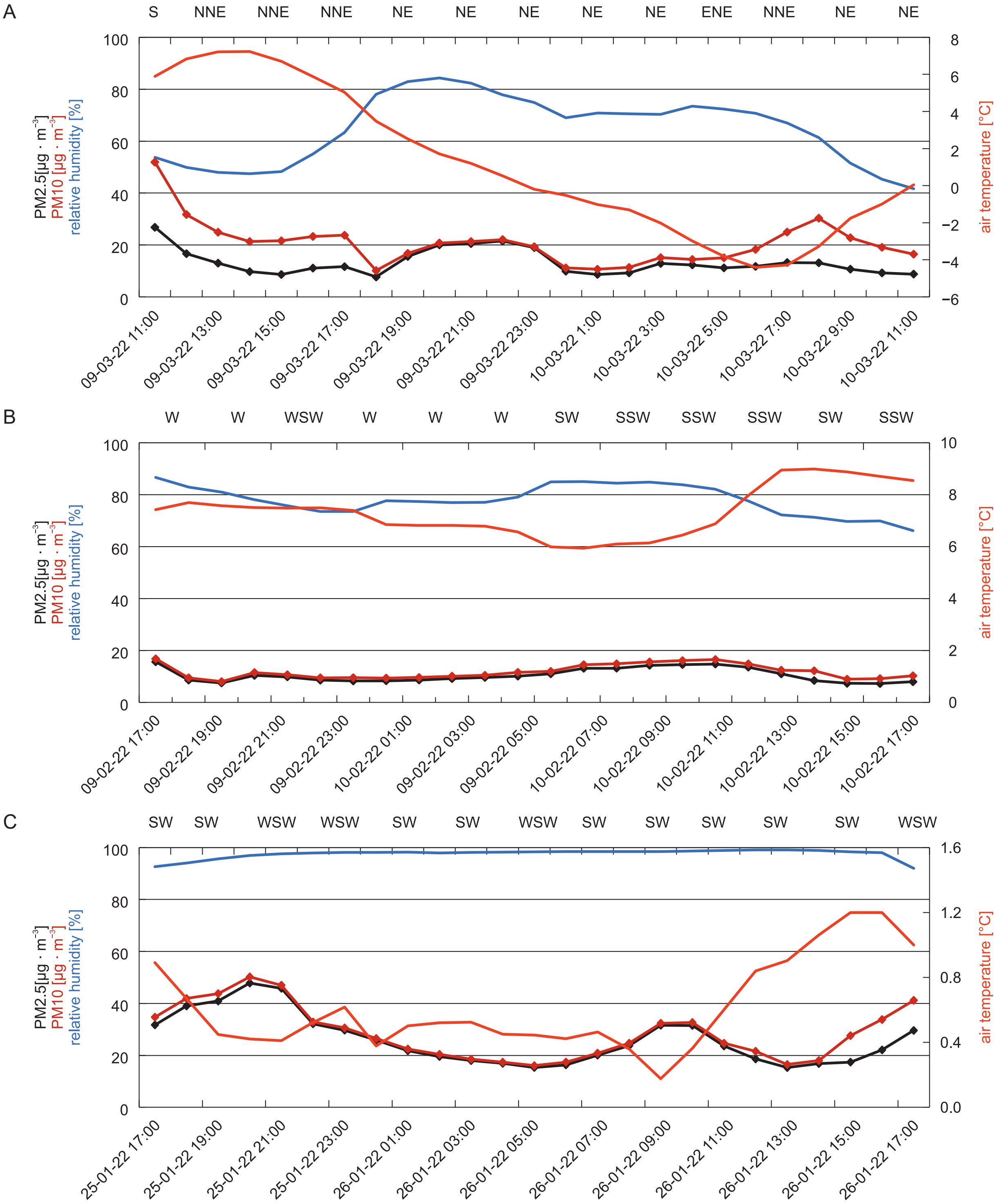

Fig. 2. Diurnal variation of $PM_{2.5}$ and PM_{10} concentrations against the background meteorological conditions at Kielce – A, Strzyżowice – B, and Katowice – C.

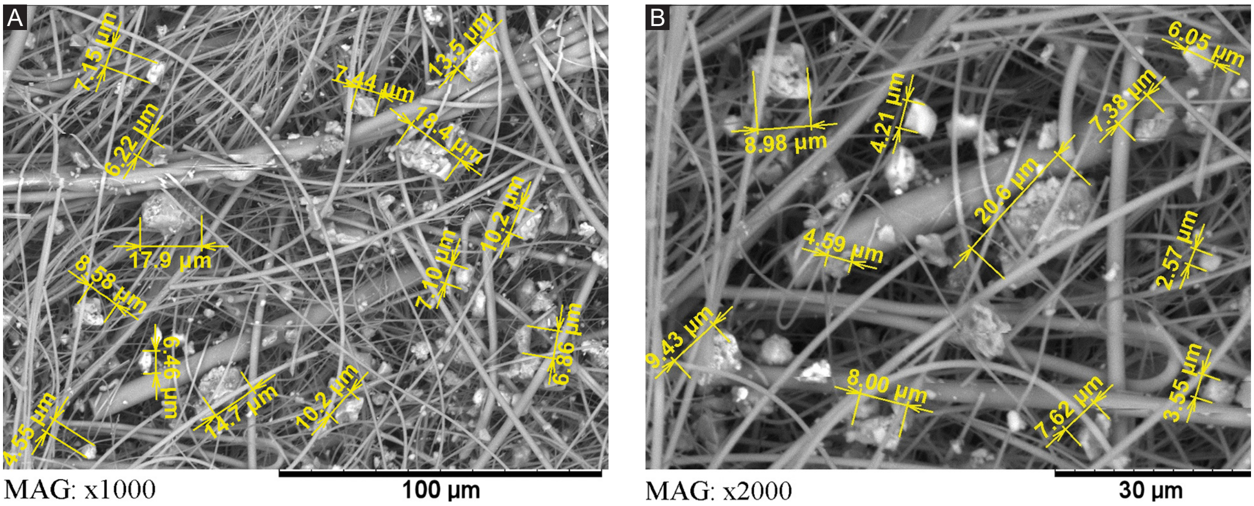

Fig. 3. Micrographs of dust sample on quartz filter from Kielce indicating the size of particles (areas A and B).

fragments were subjected to quantitative elemental analysis, focussing on selected particles of x and o type, as shown in the Figure 5A and 5B. Examples of the results are available in the bardiagrams presented below the micrographs in Figure 5 . The chemical composition (50.8% Cl, 32.8% Na) of the imaged particles and their shape (sharp-edged) indicate a significant proportion of salt particles (5x). Taking into account the location in the vicinity of the street and the time of year, it can be assumed that it is road salt used to remove snow. Much larger calcium particles (5o) indicate the presence of limestone dust (13.5% Ca), quite common in the impact zone of the Białe Zagłębie in the Świętokrzyskie Mountains (Szwed et al. 2020).

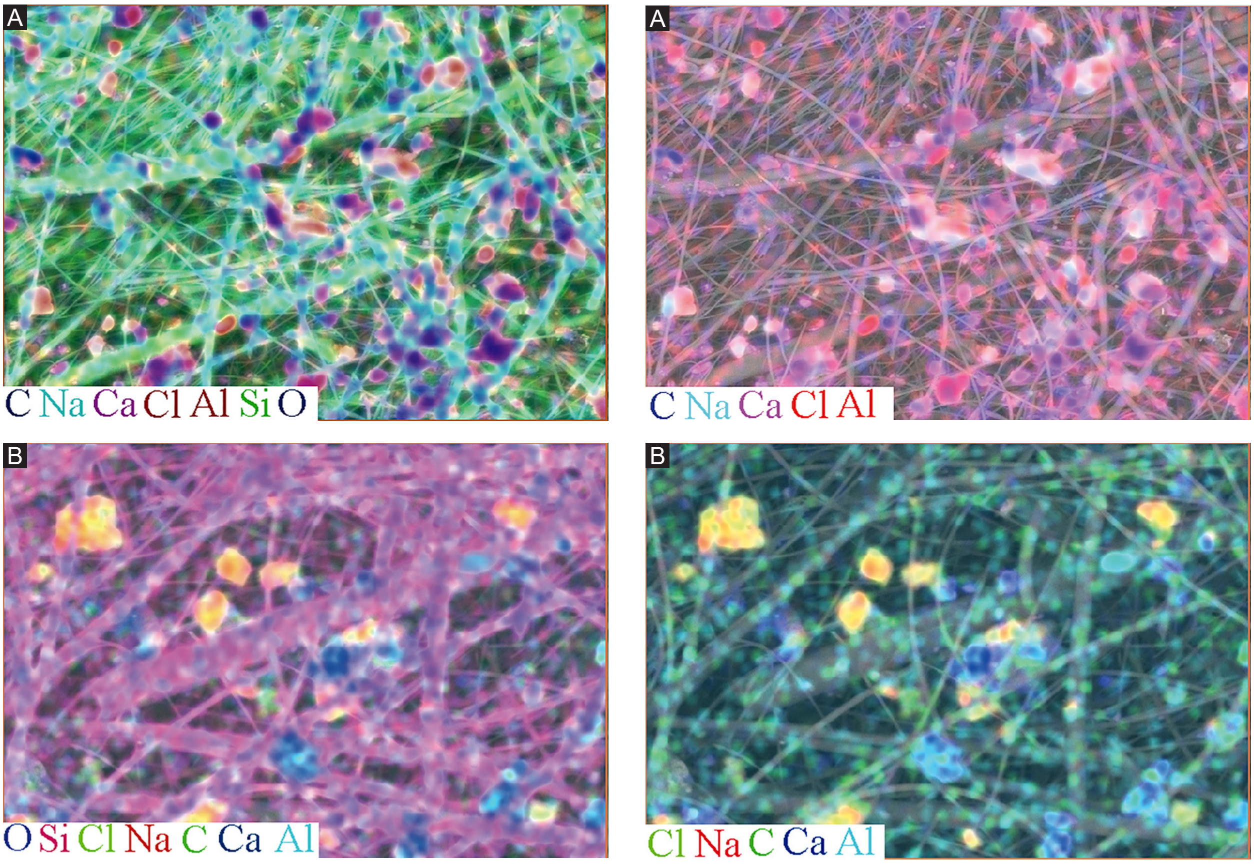

Fig. 4. EDS analysis, the distribution of signals to the elements forming dust particles (areas A and B).

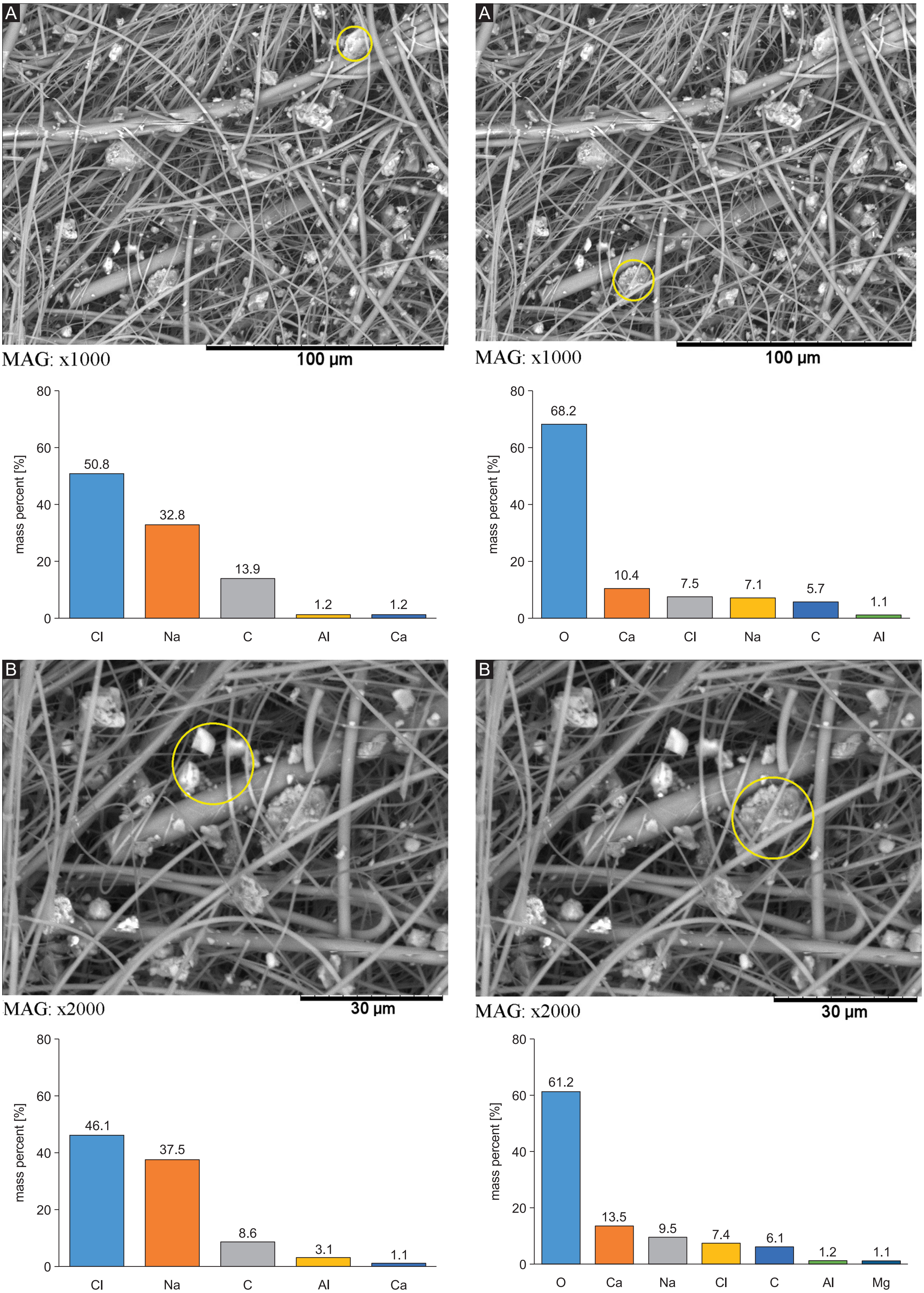

Fig. 5. Decomposition of signals into elements forming dust particles (areas A and B).

Discussion

The obtained results indicate that the permissible concentrations of $PM_{2.5}$ for 24 h (Dziennik Ustaw 2021), namely the threshold of 15 μg · m^{-3}, were exceeded (WHO 2021). The highest $PM_{2.5}$ level was observed at the industrialised area in Katowice, where it was two and three time higher than those observed at the urban (Kielce) and rural (Strzyżowice) sites, respectively. It is worth noting that measurements were conducted during different times in winter (Table 1). Katowice

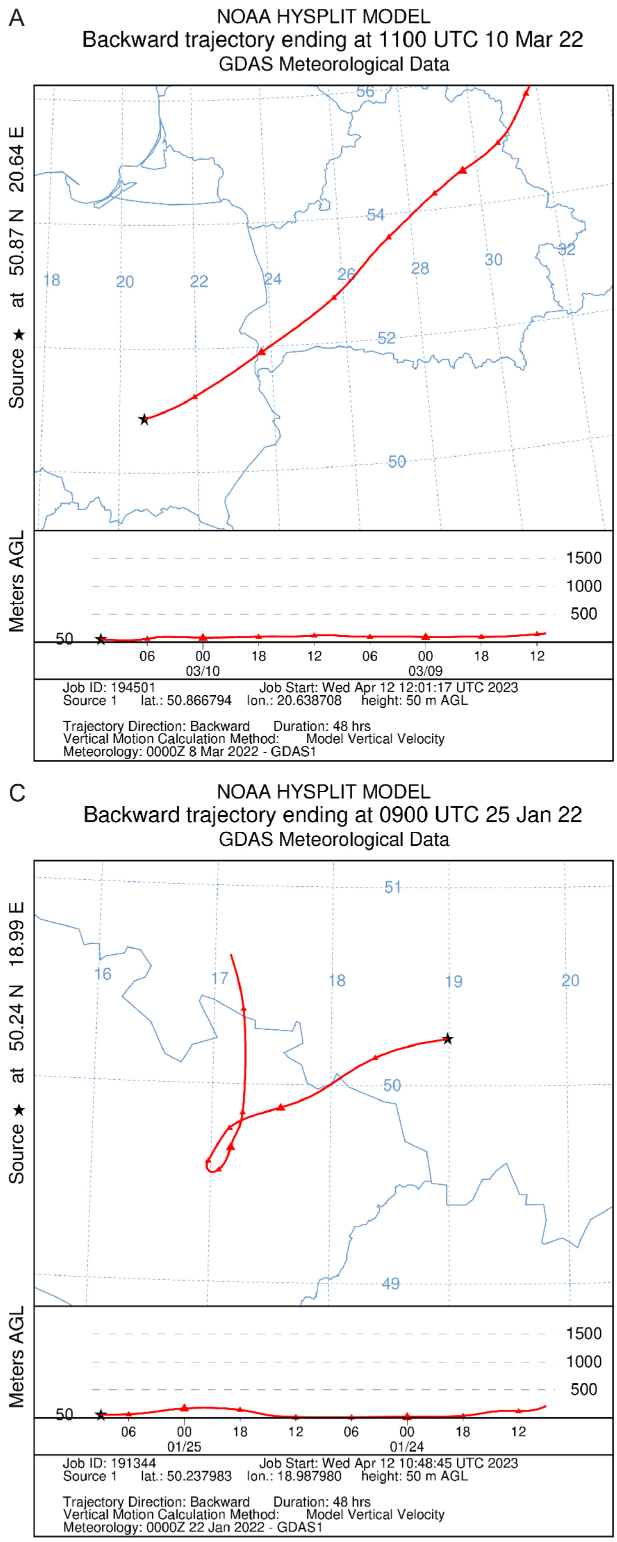

Fig. 6. Example of a HYSPLIT 48 h air mass back-trajectory arriving at Kielce – A (9th–10th March), at Strzyżowice – B (9th–10th February), and at Katowice – C (25th–26th January). Arrival height: 50 m a.g.l.

is influenced by industrial emissions, traffic and domestic activities, and measurements were conducted during a colder period (0.5 ± 0.1°C) in winter when the planetary boundary layer height is lower compared to other seasons. These conditions could lead to the worsening of atmospheric dilution as well as an atmospheric accumulation of pollutants having a local origin (Grivas et al. 2012, Mbengue et al. 2018). The BT analysis reveals recirculation of air masses over south of Poland and east of Czech Republic, covering the Silesian industrialised areas (Fig. 6C. The highest values of EC and OC were observed at Kielce, where relatively low temperature was also recorded (1.2 ± 3.9°C). Beside traffic emissions, coal and wood combustion from residential heating could promote the higher levels of EC and OC in winter, as evidenced by earlier research in the Białka Tatrzańska (where internal artificial heating is mostly achieved through the burning of coal) (Szramowiat-Sala et al. 2016). Kim et al. (2004) have documented that EC values ranged from 1.0 µg to 4.2 µg and OC values ranged from 2.2 µg to 13.5 µg in the 3 h campaign series situated in south-east of Asia. The diurnal patterns of $PM_{2.5}$ and PM_{10} at the urban (Kielce) and urban-industrial (Katowice) sites show the influence of traffic rush hour during the morning (Fig. 2A–2C). This is consistent with the higher concentrations of carbonaceous aerosols, especially EC (3.7 µg and 2.2 µg higher, respectively), associated with a lower OC/EC ratio observed at these sites compared to the rural site. In the evening and night time, the temperature is lower (Fig. 2A–2C), which could lead to enhanced emission from residential heating in winter. Therefore, the low and stable planetary boundary layer during the evening could lead to the accumulation of pollutants from local sources, including traffic, domestic activities and industries (Grivas et al. 2012, Mbengue et al. 2018).

The concentrations of carbonaceous aerosols were lowest at the rural site, and the higher OC/EC ratio observed at this site suggests a relatively higher proportion of OC, which could be attributed to the potential influence of biomass burning from residential heating and/or to the enhanced contribution of SOC associated with the transport of aged aerosols to the rural site across long distances (Mbengue et al. 2018). This is consistent with the result from BT analysis. Indeed, the air masses arriving at Kielce and Katowice were associated with lower altitude a.g.l. covering more local geographical areas (Fig. 6A and 6B), suggesting the influence of more local sources. Conversely, 48 h air masses arriving at Strzyżowice were characterised by stronger wind and higher altitude as well as a longer distance travelled commencing from north of France.

The SEM-EDS analysis of the sample from Kielce shows that the morphology and composition of the particles deposited on the quartz filters are heterogeneous. In terms of morphology, two categories were observed. The first represents particles with regular, sharp edges (salt and gypsum crystals) of considerable size up to 20 µm. Similar results were obtained in the area strongly influenced by cement and lime production (Kozłowski et al. 2019, Szwed et al. 2021). Jóźwiak and Jóźwiak (2009) carried out imaging (magnification 4000×) of the gypsum crystal on the bioindicator lichen surface, and showed a calcareous rose characteristic of this type of structures. The second category with a much smaller size of 3–10 mm is characteristic of street dust composition (Liu et al. 2019). In a study conducted on dust fall in Asia (Liu et al. 2019), a third group of particles with spherical shapes characteristic of high-temperature raw material transformations was additionally considered. The limitations of the applied research methods did not allow for the identification of this group; however, previous studies have confirmed the presence of ferro-silicate spheres in the Świętokrzyskie Mountains (Kozłowski 2013, Szwed et al. 2021).

Summary

In this pilot study, atmospheric aerosols have been characterised at urban and/or industrial, and rural, sites in Poland. The concentrations of $PM_{2.5}$, PM_{10} and carbonaceous fractions (OC and EC) were significantly higher at Katowice and Kielce, likely a result of the influence of the proximity of the anthropogenic sources (traffic, domestic activities and industries), compared to the rural site (Strzyżowice). The meteorological conditions in winter (cold weather and low and stable boundary layer) could promote the accumulation of air pollutants emitted from local sources. SEM-EDS analysis of samples from the urban site confirms the presence of internally mixed particles characteristic of anthropogenic pollutants during the heating season, including carbon and sodium chloride from winter road maintenance. Gypsum particles, typical for dust pollution, were also revealed by the examination, and are thought to have arisen consequent to transport from the area of the Białe Zagłębie, located about 30 km south-west of Kielce. This study was conducted based on 24 h measurement data. Therefore, further field investigations based on long-term measurement covering different seasons are needed to better characterise the composition and sources of atmospheric aerosols from Katowice, Kielce and Strzyżowice.

Acknowledgements

This work was financed by Jan Kochanowski University, project No. SUPB.RN.21.258 and SUPB.RN.23.093. This work was supported by the Ministry of Education, Youth and Sports of CR within the CzeCOS programme, grant No. LM2023048, and the European Regional Development Fund-Project ACTRIS-CZ, grant No. LM2023030.

The authors would like to thank the reviewers for their useful comments, which helped to improve the final version of the paper.

Author's contribution

Conceptualisation: MSz; data curation: MSz, RK, WŻ, SM, LS and RP; formal analysis: MSz, RK, WŻ, SM, LS and RP; funding acquisition: MSz, RK, MS, LS and RP; investigation: MSz, RK, WŻ, MS, LS and RP; methodology: MSz; project administration: MSz; resources: MSz; software: MSz; supervision: MSz; validation: MSz, SM and WŻ; visualisation: MSz; roles/writing – original draft: MSz; writing – review & editing: MSz, RK, WŻ, SM and LS.

References

Arndt J., Deboudt K., Anderson A., Blondel A., Eliet S., Flament P., Fourmentin M., Healy R.M., Savary V., Setyan A., Wenger J.C., 2016. Scanning electron microscopy-energy dispersive X-ray spectrometry (SEM-EDX) and aerosol time-of-flight mass spectrometry (ATOFMS) single particle analysis of metallurgy plant emissions. *Environmental Pollution* 210: 9–17. DOI 10.1016/j.envpol.2015.11.019.

Cavalli F., Viana M., Yttri K.E., Genberg J., Putaud J.-P., 2010. Toward a standardized thermal-optical protocol for measuring atmospheric organic and elemental carbon: The EUSAAR protocol. *Atmospheric Measurement Techniques* 3: 79–89. DOI 10.5194/amt-3-79-2010.

Cichowicz R., Wielgosiński G., Fetter W., 2017. Dispersion of atmospheric air pollution in summer and winter season. *Environmental Monitoring and Assessment* 189(12): 605. DOI 10.1007/S10661-017-6319-2.

Eguiluz-Gracia I., Mathioudakis A.G., Bartel S., Vijverberg S.J.H., Fuertes E., Comberiati P., Cai Y.S., Tomazic P.V., Diamant Z., Vestbo J., Galan C., Hoffmann B., 2020. The need for clean air: The way air pollution and climate change affect allergic rhinitis and asthma. *Allergy* 75(9): 2170–2184. DOI 10.1111/ALL.14177.

Grivas G., Cheristanidis S., Chaloulakou A., Koutrakis P., Mihalopoulos N., 2012. Elemental composition and source apportionment of fine and coarse particles at traffic and urban background locations in Athens, Greece. *Aerosols and Air Quality Reaserch* 18(7): 1642–1659. DOI 10.4209/aaqr.2017.12.0567.

GUS (Główny Urząd Statystyczny). Online: https://stat.gov.pl/ (accessed 23 June 2022).

Jóźwiak M.A., Jóźwiak M., 2009. Influence of cement industry on accumulation of heavy metals in bioindicators. *Ecological Chemistry and Engineering S* 16(3): 323–334.

Kampa M., Castanas E., 2008. Human health effects of air pollution. *Environmental Pollution* 151(2): 362–367. DOI 10.1016/j.envpol.2007.06.012.

Kim K.W., He Z., Kim Y., 2004. Physicochemical characteristics and radiative properties of Asian dust particles observed at Kwangju, Korea, during the 2001 ACE-Asia intensive observation period. *Journal of Geophysical Research* 109: 1–15. DOI 10.1029/2003JD003693.

Kozłowski R., 2013. Funkcjonowanie wybranych geoekosystemów Polski w warunkach zróżnicowanej antropopresji na przykładzie gór niskich i pogórza. *Landform Analysis* 23: 1–150.

Kozłowski R., Szwed M., Żukowski R., 2019. Pine needles as bioindicator of pollution by trace elements from cement-limestone industry in centraleastern Poland. *Carpathian Journal of Earth and Environmental Sciences* 14: 541–549. DOI 10.26471/cjees/2019/014/102.

Liu H., Yan Y., Chang H., Chen H., Liang L., Liu X., Qiang X., Sun Y., 2019. Magnetic signatures of natural and anthropogenic sources of urban dust aerosol. *Atmospheric Chemistry Physics* 19: 731–745. DOI 10.5194/ACP-19-731-2019.

Mbengue S., Alleman L.Y., Flament P., 2014. Size-distributed metallic elements in submicronic and ultrafine atmospheric particles from urban and industrial areas in northern France. *Atmospheric Research* 135–136: 35–47. DOI 10.1016/j.atmosres.2013.08.010.

Mbengue S., Alleman L.Y., Flament P., 2017. Metal-bearing fine particle sources in a coastal industrialized environment. *Atmospheric Research* 183: 202–211. DOI 10.1016/j.atmosres.2016.08.014.

Mbengue S., Alleman L.Y., Pascal F., 2015. Bioaccessibility of trace elements in fine and ultrafine atmospheric particles in an industrial environment. *Environmental Geochemistry and Health* 35: 875–889. DOI 10.1007/s10653-015-9756-2.

Mbengue S., Fusek M., Schwarz J., Vodička P., Šmejkalová A.H., Holoubek I., 2018. Four years of highly time resolved measurements of elemental and organic carbon at a rural background site in Central Europe. *Atmospheric Environment* 182: 335–346.

Obwieszczenie Ministra Klimatu i Środowiska z dnia 12 kwietnia 2021 r. w sprawie ogłoszenia jednolitego tekstu rozporządzenia Ministra Środowiska w sprawie poziomów niektórych substancji w powietrzu, 2021. Dziennik Ustaw poz.845.

Paraschiv L.S., Serban A., Paraschiv S., 2019. Calculation of combustion air required for burning solid fuels (coal/biomass/solid waste) and analysis of flue gas composition. *Energy Reports* 6: 36–45. DOI 10.1016/j.egyr.2019.10.016.

PCA [Polskie Centrum Akredytacji], 2021. *Zakres akredytacji laboratorium badawczego nr AB 1622, Polskie Centrum Akredytacji*, Warszawa. Online: https://lmr.ujk.edu.pl/files/Z_AB%201622_zakres_30.08.2021.pdf (accessed 23 June 2022).

Peel J., Haeuber R., Garcia V., Russell A., Neas L., 2012. Impact of nitrogen and climate change interactions on ambient air pollution and human health. *Biogeochemistry* 114: 121–134. DOI 10.1007/s10533-012-9782-4.

Rolph G., Stein A., Stunder B., 2017. Real-time environmental applications and display system: READY. *Environmental Modelling and Software* 95: 210–228. DOI 10.1016/j.envsoft.2017.06.025.

Rybiński P., Syrek B., Szwed M., Bradło D., Żukowski W., Marzec A., Śliwka-Kaszyńska M., 2021. Influence of thermal decomposition of wood and wood-based materials on the state of the atmospheric air. Emissions of toxic compounds and greenhouse gases. Energies 14(11): 3247. DOI 10.3390/en14113247.

Seinfeld J.H., 2003. Tropospheric chemistry and composition: Aerosols/particles. *Encyclopedia of Atmospheric Sciences* 54: 2349–2354. DOI 10.1016/B978-0-12-382225-3.00438-2.

Stein A.F., Draxler R.R., Rolph G.D., Stunder B.J.B., Cohen M.D., Ngan F., 2015. NOAA's HYSPLIT atmospheric transport and dispersion modeling system. *Bulletin of the American Meteorological Society* 96: 2059–2077. DOI 10.1175/BAMS-D-14-00110.1.

Szramowiat-Sala K., Styszko K., Kistler M., Kasper-Giebl A., Golas A., 2016. Carbonaceous species in atmospheric aerosols from the Krakow area (Malopolska District): Carbonaceous species dry deposition analysis. *E3S Web of Conferences* 10: 1-8. DOI 10.1051/e3sconf/20161000092.

Szwed M., Kozłowski R., Żukowski W., 2020. Assessment of air quality in the south-western part of the Świętokrzyskie Mountains based on selected indicators. Forests 11(5): 499. DOI 10.3390/f11050499.

Szwed M., Żukowski W., Kozłowski R., 2021. The presence of selected elements in the microscopic image of pine needles as an effect of cement and lime pressure within the region of Białe Zagłębie (Central Europe). Toxics 9(1): 15. DOI 10.3390/toxics9010015.

Turpin B.J., Saxena P., Andrews E., 2000. Measuring and simulating particulate organics in the atmosphere: Problems and prospects. *Atmospheric Environment* 34(18): 2983–3013. DOI 10.1016/S1352-2310(99)00501-4.

WHO (World Health Organisation), 2021. Particulate matter (PM 2.5 and PM 10), ozone, nitrogen dioxide, sulphur dioxide and carbon monoxide. World Health Organisation. Online: https://apps.who.int/iris/handle/10665/345329 (accessed 23 June 2022).